

Supplementary Information

Molecular self-assembly of 1D linear and 2D T-shape polyiodide arrangements in two organic ammonium triiodide salts: Supramolecular structures and density functional theory-based optical properties

Monia Hamdouni,^a Chakib Hrizi,^{b,*} Mohsen Ouled Mohamed Esghaier,^a Michael Knorr,^c Carsten Strohmann,^d and Slaheddine Chaabouni^a

^a Laboratoire des Sciences des Matériaux et de l'Environnement, Faculté des Sciences de Sfax, Université de Sfax, BP 1171, 3000 Sfax, Tunisia.

^b Unité de recherche Electrochimie, Matériaux et Environnement (UR17ES45), Faculté des Sciences de Gabès, Université de Gabès, Cité Erriadh, 6072 Gabès, Tunisia.

^c Institut UTINAM UMR 6213 CNRS, Université de Franche-Comté, 16, Route de Gray, 25030 Besançon, France.

^d Anorganische Chemie, Technische Universität Dortmund, Otto-Hahn Straße 6, 44227 Dortmund, Germany.

Corresponding Author, Email: h_chakib1212@yahoo.fr

Table of contents

1. Materials

2. FT-IR spectroscopy of $\text{C}_7\text{H}_{11}\text{N}_2^+\cdot\text{I}_3^-\cdot 0.5\text{H}_2\text{O}$ (**1**) and $(\text{C}_2\text{H}_5)_4\text{NI}_3$ (**2**)

Figure S1. Hirshfeld surfaces, total and detailed composed 2D fingerprint plots (FP) of cationic units in compound **1**, $\text{C}_7\text{H}_{11}\text{N}_2^+\cdot\text{I}_3^-\cdot 0.5\text{H}_2\text{O}$.

Figure S2. Hirshfeld surfaces, total and detailed composed 2D fingerprint plots (FP) of anionic units in compound **1**, $\text{C}_7\text{H}_{11}\text{N}_2^+\cdot\text{I}_3^-\cdot 0.5\text{H}_2\text{O}$.

Figure S3. Hirshfeld surfaces, total and detailed composed 2D fingerprint plots (FP) of water molecule in compound **1**, $\text{C}_7\text{H}_{11}\text{N}_2^+\cdot\text{I}_3^-\cdot 0.5\text{H}_2\text{O}$.

Figure S4. Hirshfeld surfaces, total and detailed composed 2D fingerprint plots (FP) of cationic units in compound **2**, $(\text{C}_2\text{H}_5)_4\text{NI}_3$.

Figure S5. Hirshfeld surfaces, total and detailed composed 2D fingerprint plots (FP) of anionic units ((I1–I2–I3) fragment) in compound **2**, $(\text{C}_2\text{H}_5)_4\text{NI}_3$.

Figure S6. Hirshfeld surfaces, total and detailed composed 2D fingerprint plots (FP) of anionic units ((I4A–I5A–I6A / I4B–I5B–I6B) fragment) in compound **2**, $(\text{C}_2\text{H}_5)_4\text{NI}_3$.

Figure S7. IR spectrum of the compound **1**, $\text{C}_7\text{H}_{11}\text{N}_2\text{I}_3\cdot 0.5\text{H}_2\text{O}$.

Figure S8. IR spectrum of the compound **2**, $(\text{C}_2\text{H}_5)_4\text{NI}_3$.

Figure S9. TG and dTG measurements results for **1** and **2**.

Figure S10. Type and shapes of selected frontier molecular orbitals (MOs) of **1** and **2** in a vacuum by TD-DFT method.

Table S1. Selected geometric parameters (\AA , $^\circ$) for compounds (**1**) and (**2**).

Table S2. Hydrogen bonds geometry (\AA , $^\circ$) for the **1** and **2** compounds.

Table S3. Assignments of the infrared bands for the compounds **1** and **2**.

3. References

1 Materials

SbI₃, hydroiodic acid, methanol, ethanol, 4-Dimethylaminopyridine and Tetraethylammonium iodide were commercially obtained from Sigma Aldrich and Acros.

2 FT-IR spectroscopy of C₇H₁₁N₂⁺.I₃⁻.0.5H₂O (1) and (C₂H₅)₄NI₃ (2)

FT-IR spectroscopy has been undertaken in order to verify the functional groups present in the crystal and to investigate their vibrational behavior in the solid state. The IR spectra measured between 400 and 4000 cm⁻¹ for the two compounds **1** and **2** are shown in Figs. S7 and S8. Results are notably analytical to the structural features of the compounds, clearly supporting the structural models refined from single-crystal X-ray diffraction. For the two compounds, tentative assignments for organic cations majority vibrational bands have been presented using previously reported data in the literature on similar compounds. Using previous works reported in the literature on similar compounds, assignments of calculated and observed infrared bands are quoted in Table S3. In this work, we tried to give most precise assignment of the observed bands on the basis on our calculations as a preliminary source in the discussion and also by comparison with the previously reported vibrational studies of similar compounds.

For compound **1**, the presence of water molecule gives rise in high frequencies to the appearance of a broad band at 3450 cm⁻¹ which correspond to typical stretching $\nu(\text{O-H})$ vibration. The two absorption bands located at 3290 and 3120 cm⁻¹ correspond to symmetrical stretching modes $\nu(\text{N-H})$ of 4-(Dimethylamino) pyridinium cations.¹ The bands ranging from 2970 to 2600 cm⁻¹ are due to the stretching vibration frequencies of C–H in the aromatic rings and the methyl groups.² The C–N stretching bands lie at 2350, 2000 cm⁻¹.³ The band at 1680 cm⁻¹ is assigned to the N-H and O-H bending modes.¹ The bands at 1560 and 1400 cm⁻¹ are attributable to the C–N and C=C asymmetric stretching modes for the pyridine.² The absorption band located at 1210 cm⁻¹ corresponds to the $\nu(\text{C-N})$ and $\nu(\text{C-C})$ modes.¹ The band at 995 cm⁻¹ can be attributed to the $\delta(\text{C-C})$ mode.¹ The remaining bands in the range 890 to 490 cm⁻¹ are assigned to $\gamma(\text{C-C})$, $\gamma(\text{C-H})$ and $\gamma(\text{C-N})$ out-of-plane bending modes.

For compound **2**, a wide band observed at 3454 cm⁻¹ was assigned to the water adsorbed by KBr during the pellet preparation. A succession of bands were then observed in the 3006–2595 cm⁻¹ spectral range and were assigned to the asymmetric and symmetric stretching modes of the CH₃ and CH₂ groups.^{4,5} The weak band observed around 2258 cm⁻¹ was assigned to a non-fundamental mode corresponding probably either to a combination mode involving the $\nu_{\text{as}}(\text{C-N})$ stretching and CH₂ twisting modes or to the harmonic of the r(CH₃)

mode.⁴ A very intense band has been observed at 1451 cm⁻¹, characterising the CH₃ group assymetric bending mode. Three successive bands rising at respectively 1393, 1370 and 1269 cm⁻¹ are ascribed to the symmetric bending mode of methyl groups. The band observed at 1179 cm⁻¹ corresponds to CH₃ rocking mode and to the (C–C)₄N⁺ skeletal stretching modes. The bands at 1114 and 1076 cm⁻¹ can be attributed to the C–C asymmetric stretching mode. The presence of bands at 1025 and 996 cm⁻¹ is due to C–N asymmetric stretching mode. The C–N symmetric stretching mode is detected at 782 cm⁻¹. The bands corresponding to the CH₂ rocking modes and to the tetraethylammonium skeletal bending modes were all observed at 893cm⁻¹. It is worth noting that the band corresponding to the tetraethylammonium skeletal asymmetric δ_{as} (C–C–N) and symmetric δ_s (C–C–N) bending are present respectively at 666 and 467cm⁻¹.⁴

4-(Dimethylamino) pyridinium cation

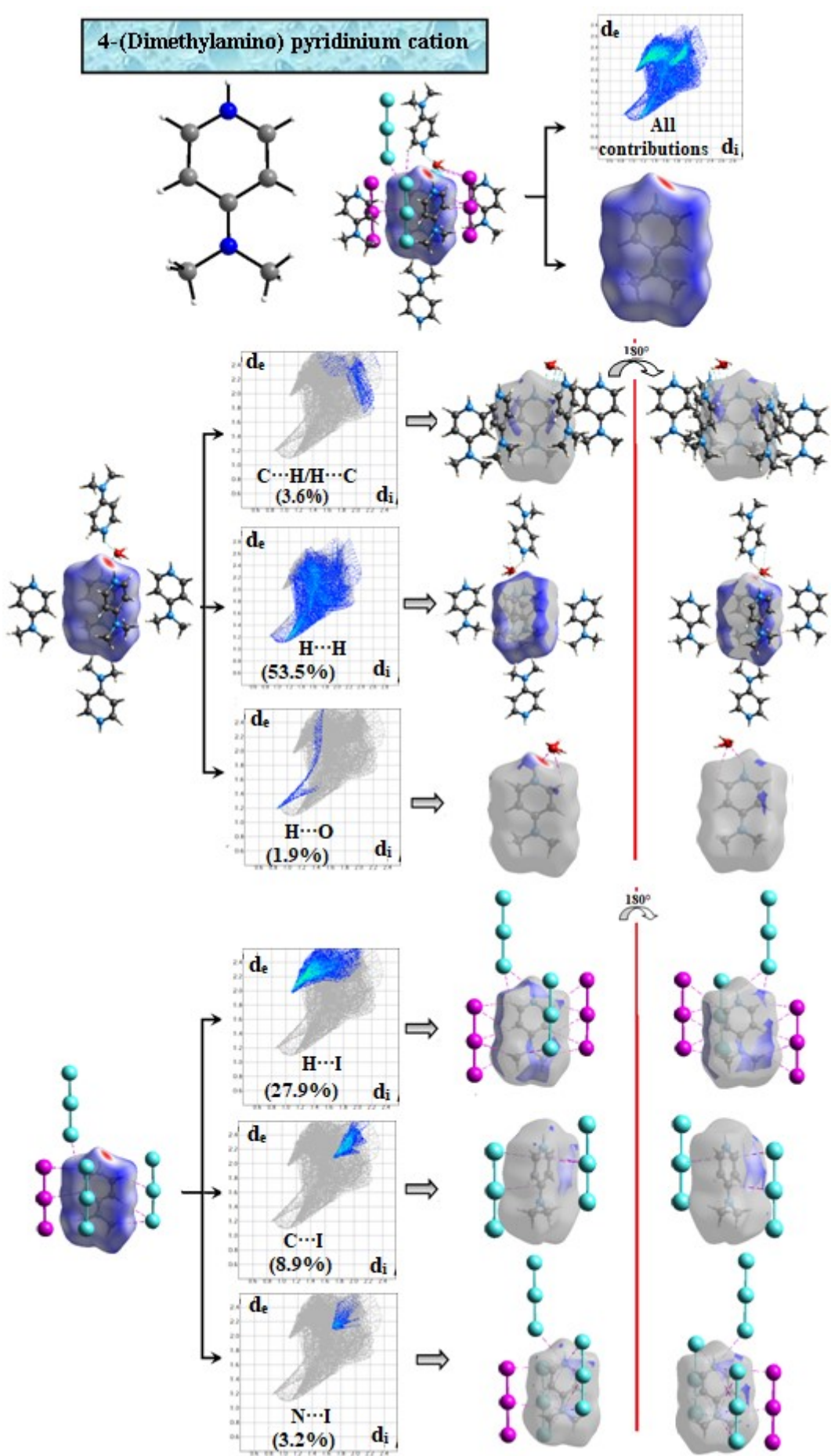


Figure S1. Hirshfeld surfaces, total and detailed composed 2D fingerprint plots (FP) of cationic units in compound **1**, $\text{C}_7\text{H}_{11}\text{N}_2^+\cdot\text{I}_3^- \cdot 0.5\text{H}_2\text{O}$.

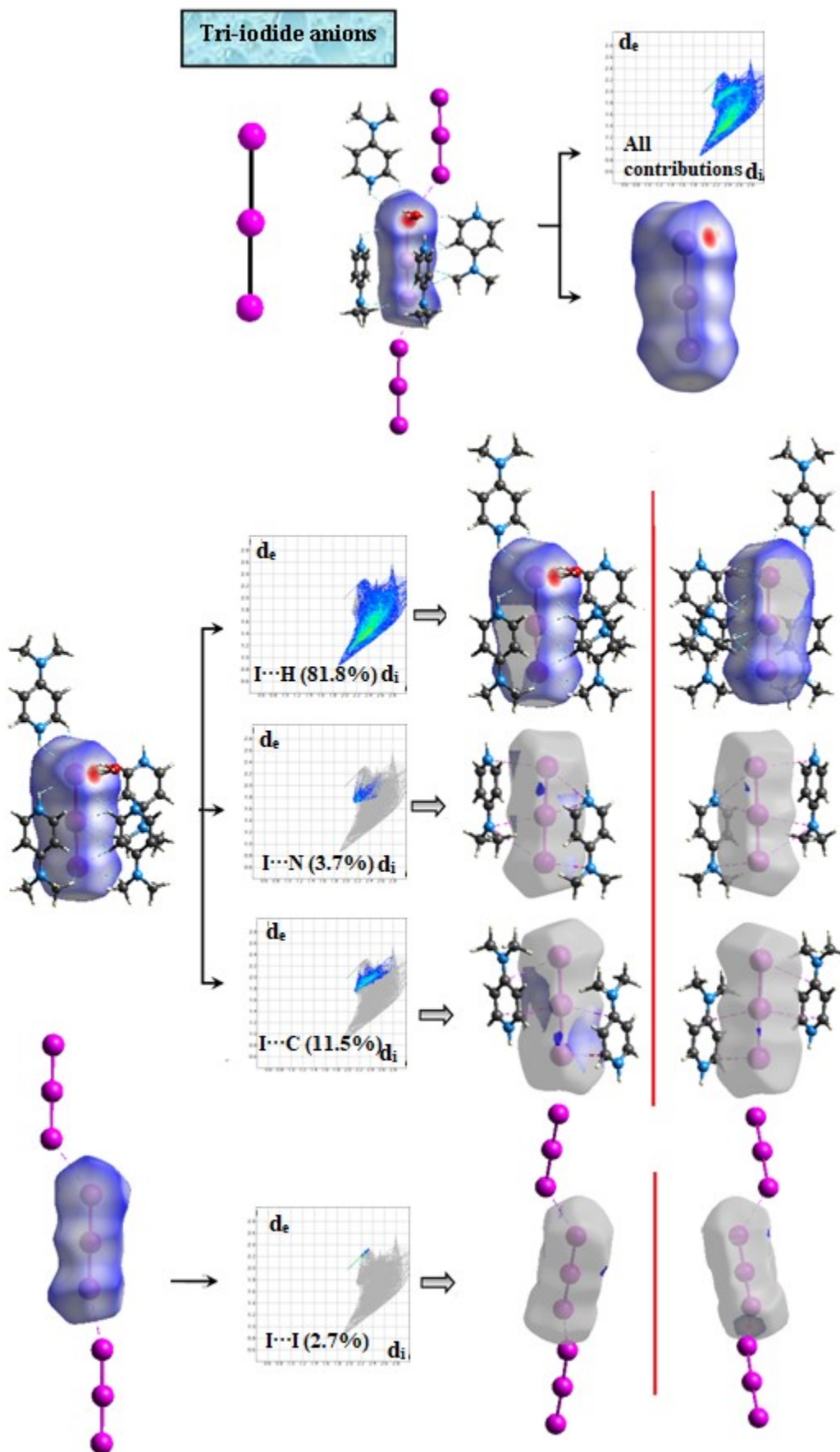


Figure S2. Hirshfeld surfaces, total and detailed composed 2D fingerprint plots (FP) of anionic units in compound **1**, $\text{C}_7\text{H}_{11}\text{N}_2^+\text{I}_3^- \cdot 0.5\text{H}_2\text{O}$.

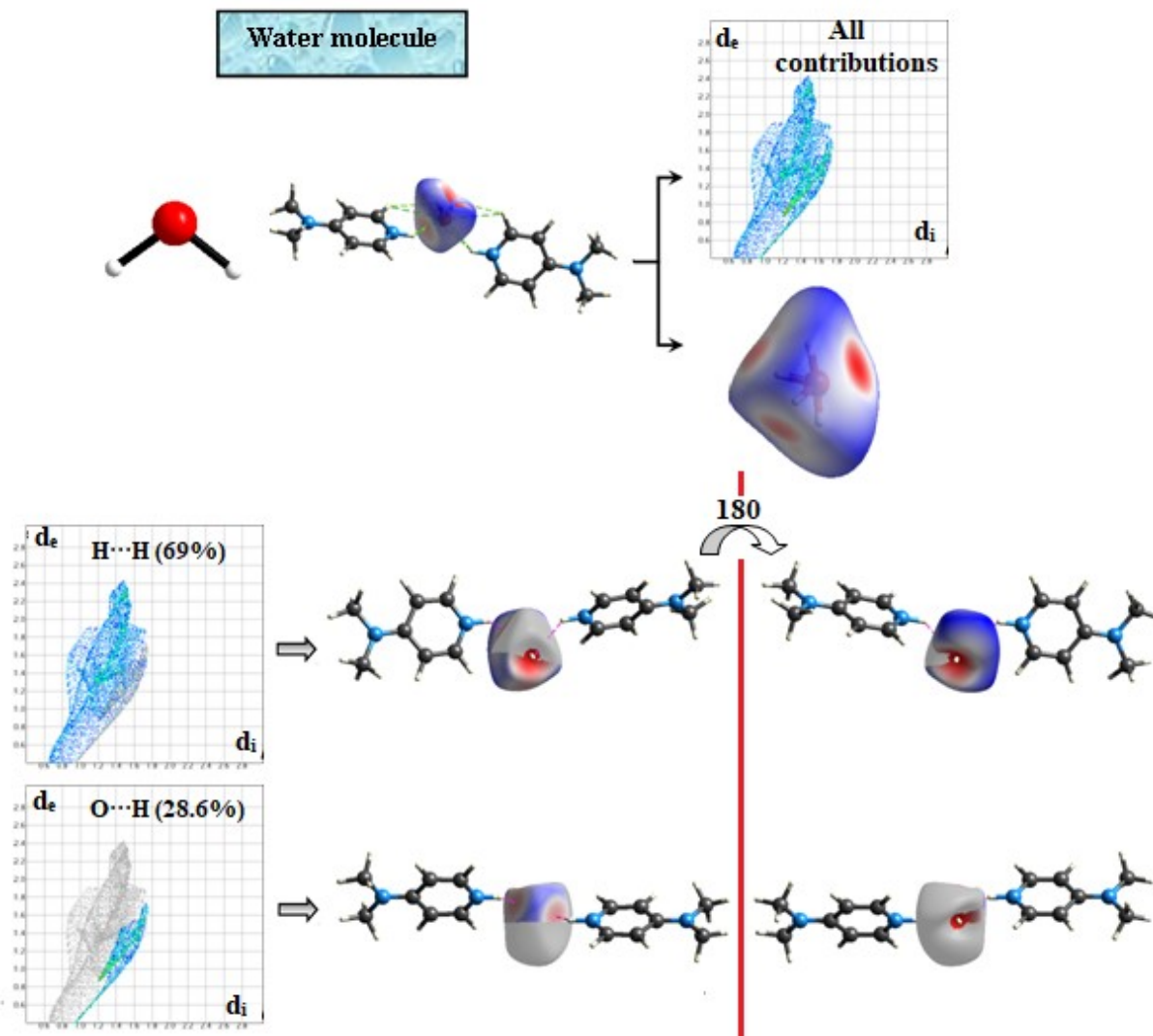


Figure S3. Hirshfeld surfaces, total and detailed composed 2D fingerprint plots (FP) of water molecule in compound **1**, $\text{C}_7\text{H}_{11}\text{N}_2^+\text{I}_3^- \cdot 0.5\text{H}_2\text{O}$.

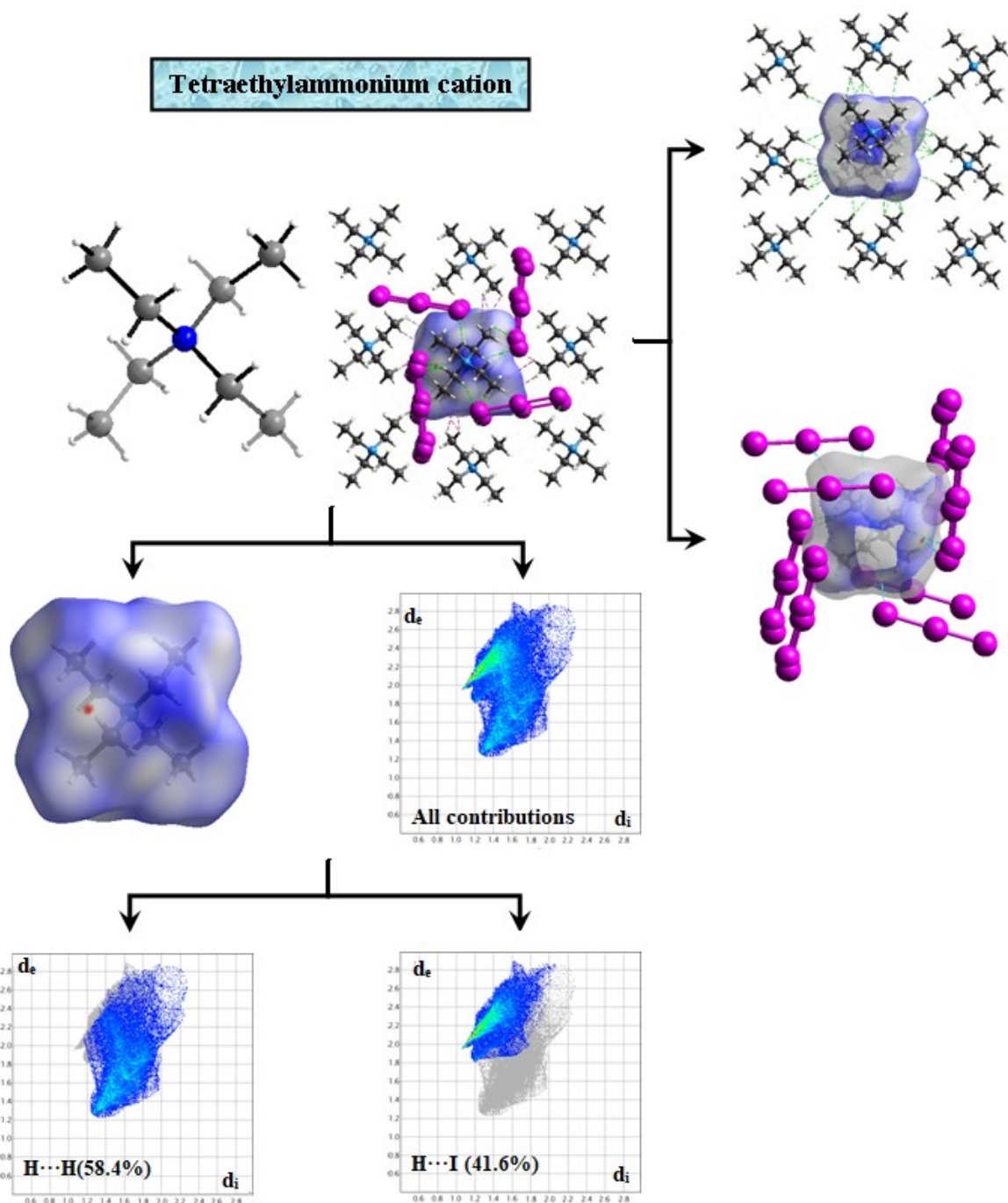


Figure S4. Hirshfeld surfaces, total and detailed composed 2D fingerprint plots (FP) of cationic units in compound 2, $(C_2H_5)_4NI_3$.

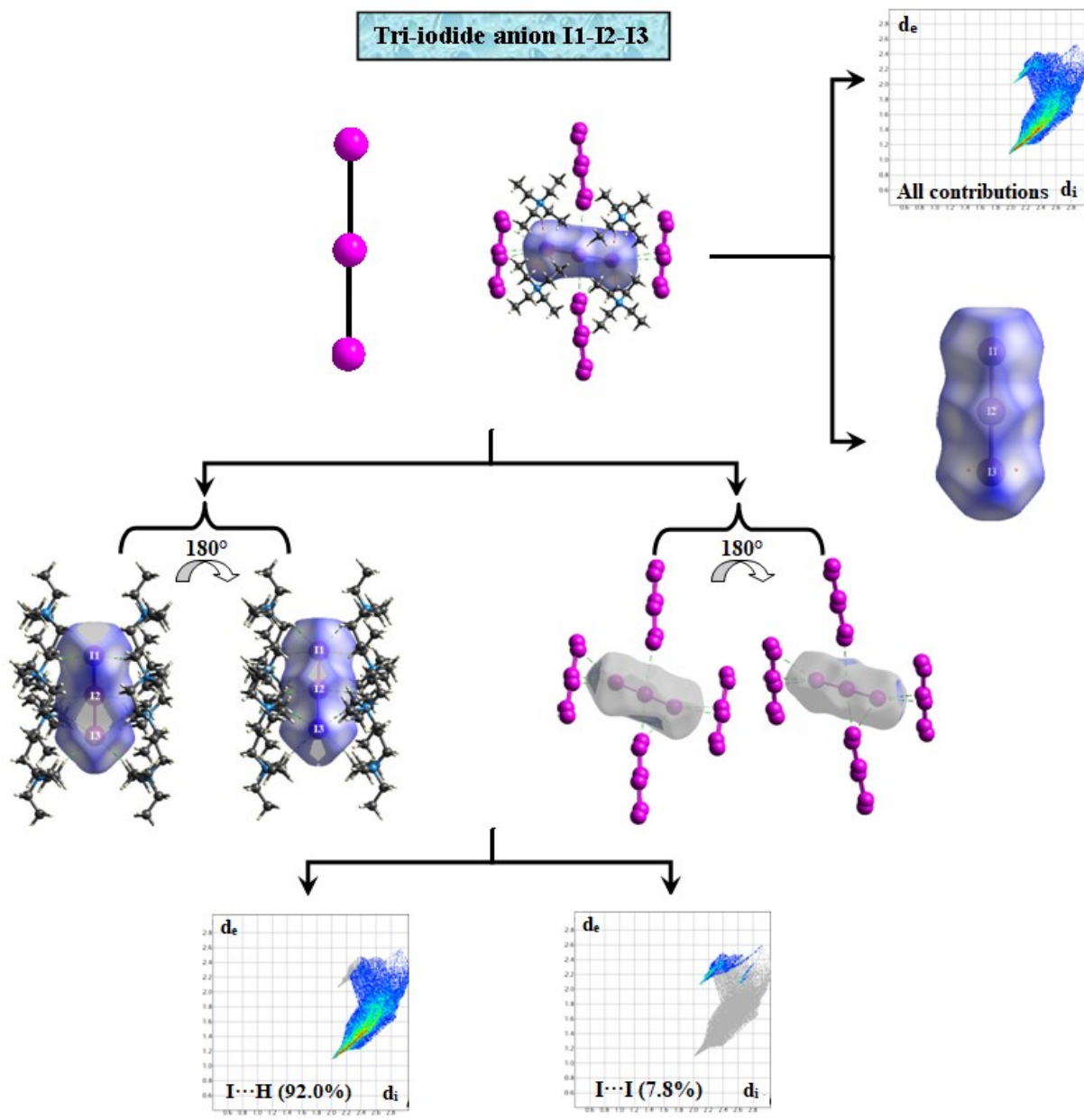


Figure S5. Hirshfeld surfaces, total and detailed composed 2D fingerprint plots (FP) of anionic units ($(\text{I}_1\text{-}\text{I}_2\text{-}\text{I}_3)$ fragment) in compound **2**, $(\text{C}_2\text{H}_5)_4\text{NI}_3$.

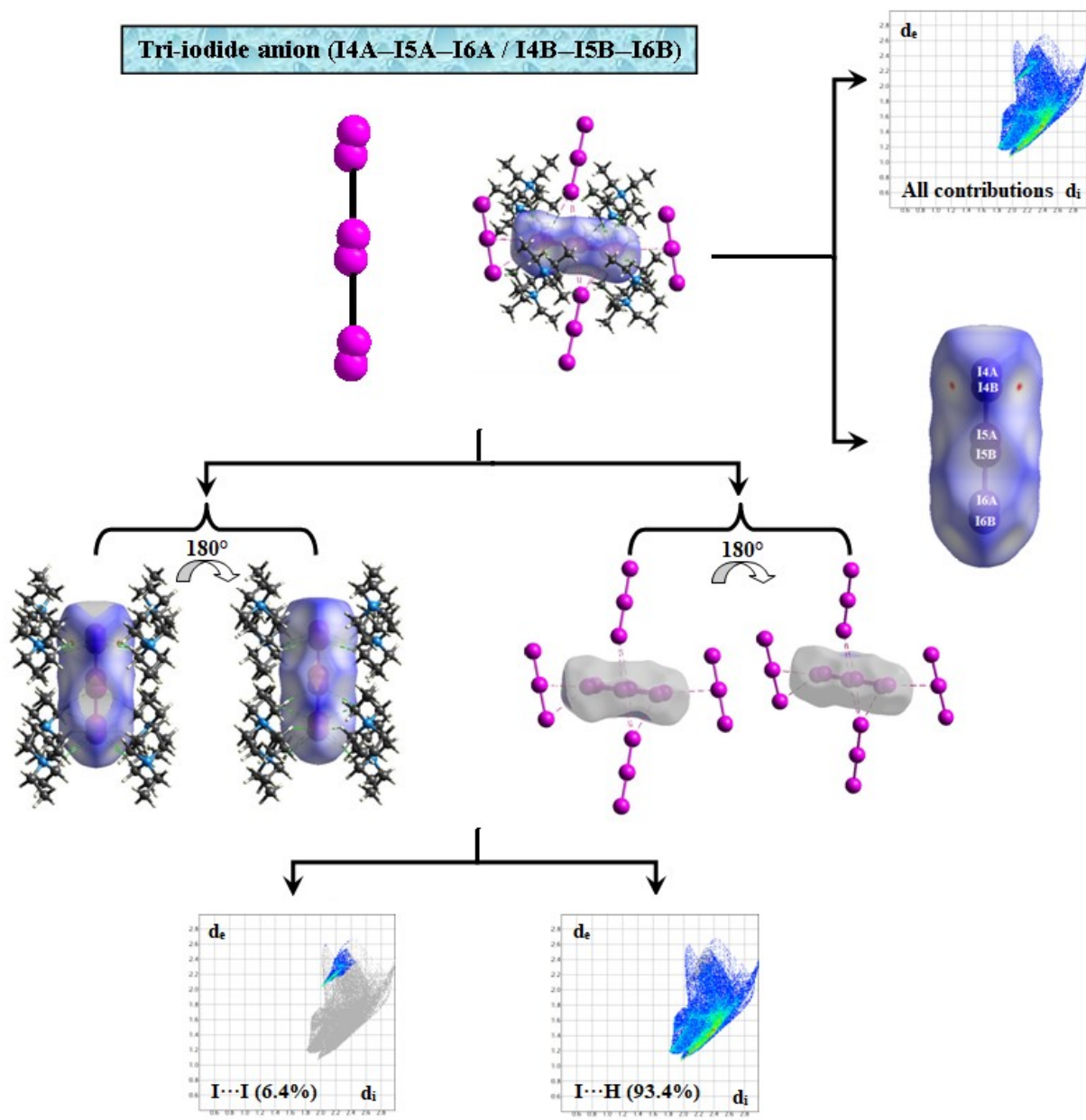


Figure S6. Hirshfeld surfaces, total and detailed composed 2D fingerprint plots (FP) of anionic units ($(\text{I}4\text{A}-\text{I}5\text{A}-\text{I}6\text{A}$ / $\text{I}4\text{B}-\text{I}5\text{B}-\text{I}6\text{B}$) fragment) in compound **2**, $(\text{C}_2\text{H}_5)_4\text{NI}_3$.

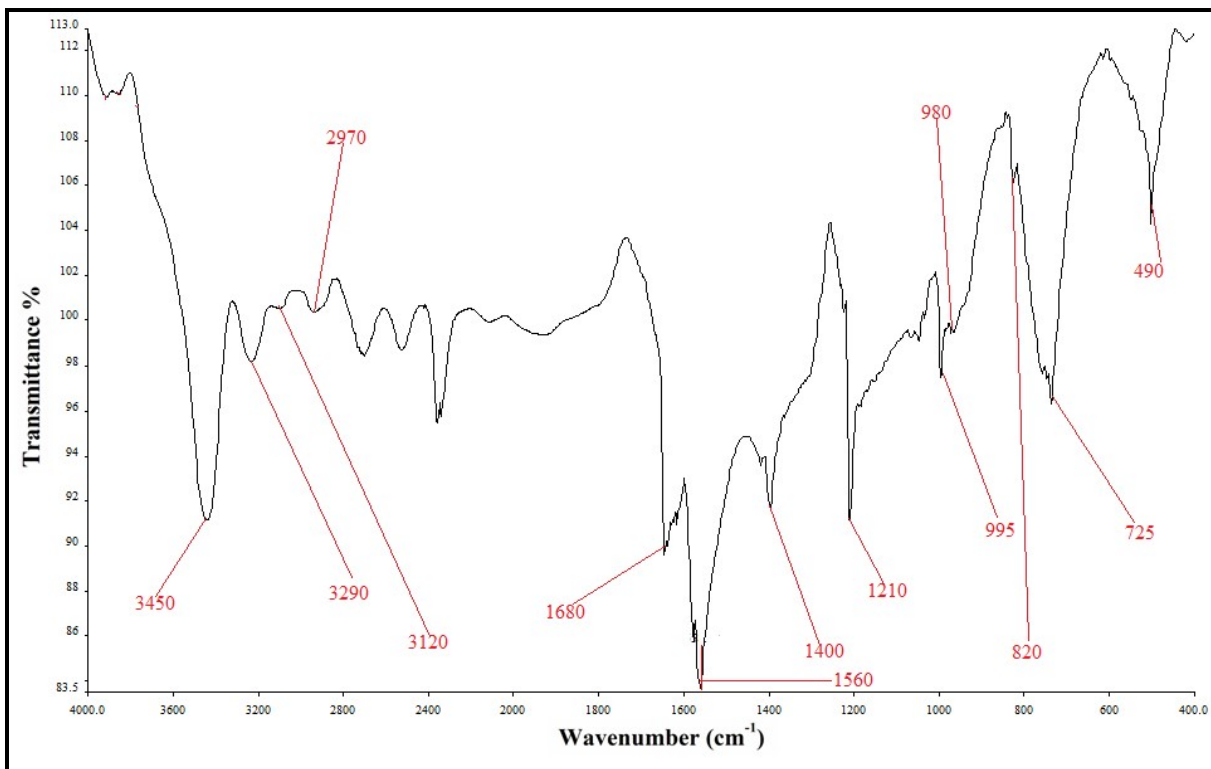


Figure S7. IR spectrum of the compound **1**, $\text{C}_7\text{H}_{11}\text{N}_2\text{I}_3 \cdot 0.5\text{H}_2\text{O}$.

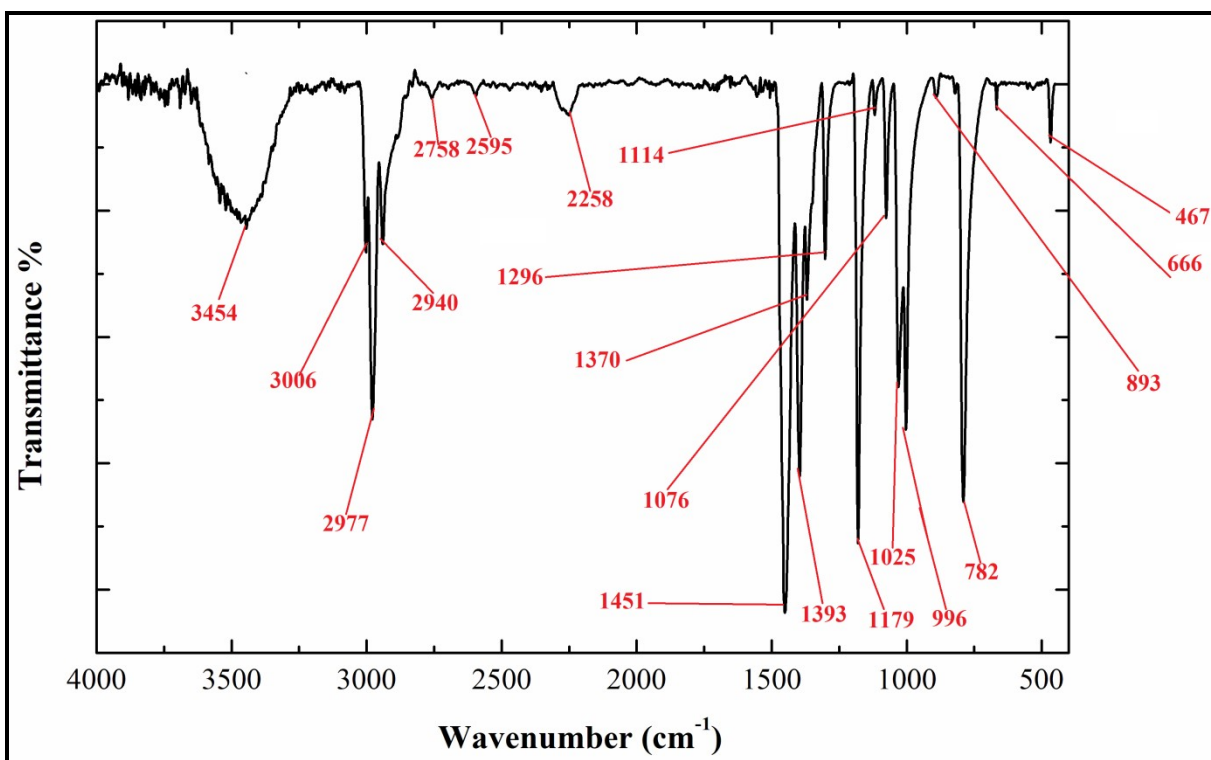


Figure S8. IR spectrum of the compound **2**, $(\text{C}_2\text{H}_5)_4\text{NI}_3$.

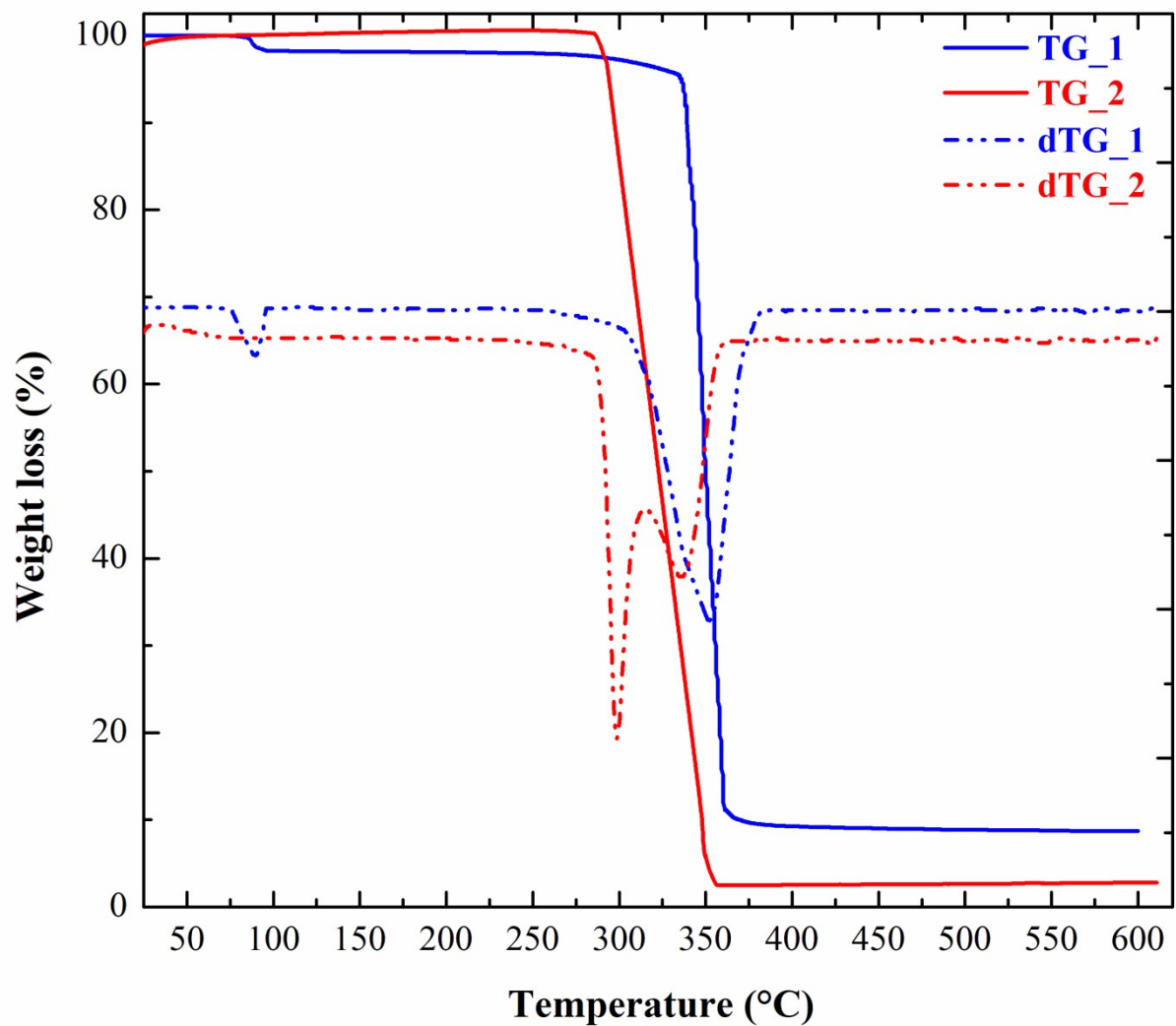


Figure S9. TG and dTG measurements results for **1** and **2**.

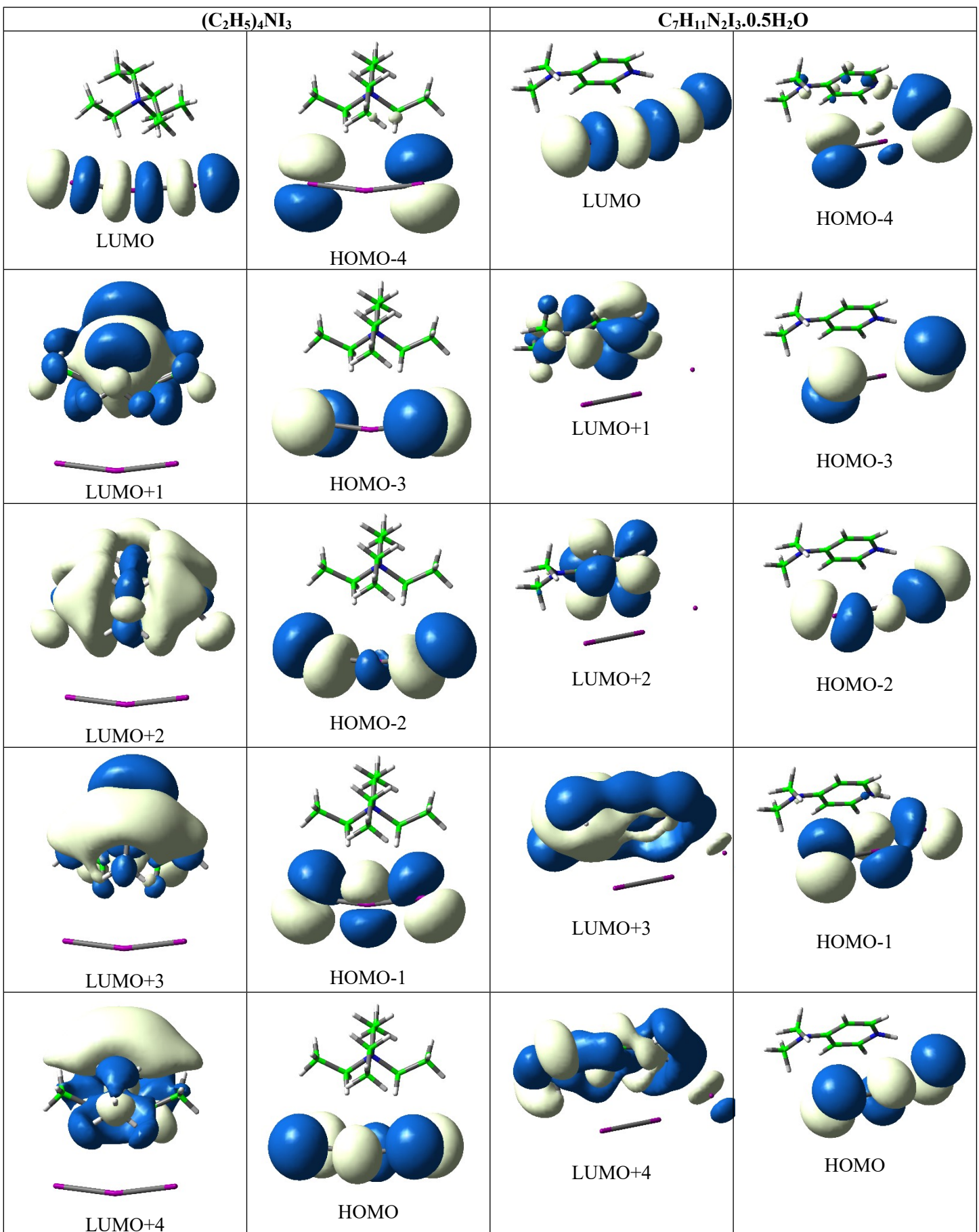


Figure S10. Type and shapes of selected frontier molecular orbitals (MOs) of **1** and **2** in a vacuum by TD-DFT method.

Table S1. Selected geometric parameters (\AA , $^\circ$) for compounds **(1)** and **(2)**.

C₇H₁₁N₂⁺.I₃⁻.0.5H₂O (1)			
I1—I2	2.8835 (9)	C1—C5	1.423 (12)
I2—I3	2.9627 (9)	C2—H2	0.9300
O1—H1A ⁱ	0.85 (2)	C2—C3	1.345 (13)
O1—H1A	0.85 (2)	C3—H3	0.9300
O1—H1B	0.85 (2)	C4—H4	0.9300
O1—H1B ⁱ	0.85 (2)	C4—C5	1.340 (13)
N1—H1	0.8600	C5—H5	0.9300
N1—C3	1.338 (12)	C6—H6A	0.9600
N1—C4	1.336 (12)	C6—H6B	0.9600
N2—C1	1.324 (11)	C6—H6C	0.9600
N2—C6	1.450 (11)	C7—H7A	0.9600
N2—C7	1.451 (11)	C7—H7B	0.9600
C1—C2	1.408 (12)	C7—H7C	0.9600
I1—I2—I3	177.83 (3)	N1—C3—H3	119.1
H1A—O1—H1A ⁱ	171 (10)	C2—C3—H3	119.1
H1A—O1—H1B ⁱ	67 (10)	N1—C4—H4	118.8
H1A—O1—H1B	104 (5)	N1—C4—C5	122.3 (9)
H1A ⁱ —O1—H1B ⁱ	104 (5)	C5—C4—H4	118.8
H1B—O1—H1A ⁱ	67 (10)	C1—C5—H5	119.9
H1B—O1—H1B ⁱ	59 (10)	C4—C5—C1	120.3 (9)
C3—N1—H1	120.3	C4—C5—H5	119.9
C4—N1—H1	120.3	N2—C6—H6A	109.5
C4—N1—C3	119.4 (8)	N2—C6—H6B	109.5
C1—N2—C6	122.3 (8)	N2—C6—H6C	109.5
C1—N2—C7	121.3 (7)	H6A—C6—H6B	109.5
C6—N2—C7	116.4 (7)	H6A—C6—H6C	109.5
N2—C1—C2	121.9 (8)	H6B—C6—H6C	109.5
N2—C1—C5	122.7 (8)	N2—C7—H7A	109.5
C2—C1—C5	115.4 (8)	N2—C7—H7B	109.5
C1—C2—H2	119.6	N2—C7—H7C	109.5
C3—C2—C1	120.8 (9)	H7A—C7—H7B	109.5
C3—C2—H2	119.6	H7A—C7—H7C	109.5
N1—C3—C2	121.8 (10)	H7B—C7—H7C	109.5
C₈H₂₀N⁺.I₃⁻ (2)			
I1—I2	2.9122 (7)	C3—H3B	0.9700
I2—I3	2.9547 (7)	C3—C4	1.505 (7)
I4A—I5A	2.8900 (10)	C4—H4A	0.9600
I5A—I6A	2.9835 (10)	C4—H4B	0.9600
I4B—I5B	2.900 (13)	C4—H4C	0.9600
I5B—I6B	2.952 (13)	C5—H5A	0.9700
N1—C1	1.504 (6)	C5—H5B	0.9700

N1—C3	1.510 (6)	C5—C6	1.497 (7)
N1—C5	1.504 (6)	C6—H6A	0.9600
N1—C7	1.511 (6)	C6—H6B	0.9600
C1—H1A	0.9700	C6—H6C	0.9600
C1—H1B	0.9700	C7—H7A	0.9700
C1—C2	1.524 (7)	C7—H7B	0.9700
C2—H2A	0.9600	C7—C8	1.539 (8)
C2—H2B	0.9600	C8—H8A	0.9600
C2—H2C	0.9600	C8—H8B	0.9600
C3—H3A	0.9700	C8—H8C	0.9600
I1—I2—I3	179.52 (2)	C3—C4—H4C	109.5
I4A—I5A—I6A	177.87 (4)	H4A—C4—H4B	109.5
I4B—I5B—I6B	179.7 (8)	H4A—C4—H4C	109.5
C1—N1—C3	111.0 (4)	H4B—C4—H4C	109.5
C1—N1—C5	106.9 (4)	N1—C5—H5A	108.3
C1—N1—C7	110.7 (4)	N1—C5—H5B	108.3
C3—N1—C7	106.4 (4)	H5A—C5—H5B	107.4
C5—N1—C3	110.9 (3)	C6—C5—N1	116.1 (4)
C5—N1—C7	111.1 (4)	C6—C5—H5A	108.3
N1—C1—H1A	108.8	C6—C5—H5B	108.3
N1—C1—H1B	108.8	C5—C6—H6A	109.5
N1—C1—C2	113.9 (4)	C5—C6—H6B	109.5
H1A—C1—H1B	107.7	C5—C6—H6C	109.5
C2—C1—H1A	108.8	H6A—C6—H6B	109.5
C2—C1—H1B	108.8	H6A—C6—H6C	109.5
C1—C2—H2A	109.5	H6B—C6—H6C	109.5
C1—C2—H2B	109.5	N1—C7—H7A	108.7
C1—C2—H2C	109.5	N1—C7—H7B	108.7
H2A—C2—H2B	109.5	N1—C7—C8	114.1 (5)
H2A—C2—H2C	109.5	H7A—C7—H7B	107.6
H2B—C2—H2C	109.5	C8—C7—H7A	108.7
N1—C3—H3A	108.4	C8—C7—H7B	108.7
N1—C3—H3B	108.4	C7—C8—H8A	109.5
H3A—C3—H3B	107.5	C7—C8—H8B	109.5
C4—C3—N1	115.4 (4)	C7—C8—H8C	109.5
C4—C3—H3A	108.4	H8A—C8—H8B	109.5
C4—C3—H3B	108.4	H8A—C8—H8C	109.5
C3—C4—H4A	109.5	H8B—C8—H8C	109.5
C3—C4—H4B	109.5		

Table S2. Hydrogen bonds geometry (\AA , $^\circ$) for the **1** and **2** compounds.

<i>Compound 1</i>					
D–H	A	d(D–H)	d(H···A)	D–H···A	d(D···A)
O1–H1A	I3 ⁱ	0.85(2)	3.08(2)	124(2)	3.634(1)
O1–H1B	I3 ⁱⁱ	0.85(2)	2.87(1)	150(2)	3.634(1)
N1–H1	O1	0.86	2.16	142.4	2.892(1)
C3–H3	I2 ⁱⁱ	0.93	3.17	139	3.916(1)
C4–H4	I3 ⁱⁱⁱ	0.93	3.27	136.9	4.001(1)
C5–H5	I2 ^{iv}	0.93	3.28	171.3	4.201(9)

Symmetry codes: *i* : -x+2, y+1, -z+1/2 ; *ii* : x, y+1, z ; *iii* : -x+2, y, -z+1/2 ; *iv* : x, -y-1, z+1/2.

<i>Compound 2</i>					
C1–H1B	I3 ^v	0.97	3.26	140.9	4.056(5)
C2–H2A	I4B ^v	0.96	3.10	129.5	3.786(1)
C3–H3A	I3	0.97	3.16	145.9	4.005(5)
C3–H3B	I6B ^{vi}	0.97	3.14	162.0	4.069(1)
C4–H4A	I2	0.96	3.31	156.3	4.208(5)
C5–H5A	I1 ^{vii}	0.97	3.23	166.5	4.177(5)
C5–H5B	I4A ^{viii}	0.97	3.15	158.4	4.064(5)
C5–H5B	I4B ^{viii}	0.97	3.18	148.3	4.035(1)
C6–H6B	I6A	0.96	3.28	163.6	4.212(6)
C6–H6B	I5B	0.96	3.31	122.2	3.902(9)
C7–H7A	I6B	0.97	3.16	136.4	3.921(1)
C7–H7B	I1	0.97	3.31	134.2	4.047(5)

Symmetry codes: *v* : -x+3/2, -y, z-1/2; *vi* : x-1/2, y, -z+1/2 ; *vii* : -x+1, y, -z+1 ; *viii* : -x+2, -y, 1-z.

Table S3. Assignments of the infrared bands for the compounds **1** and **2**.

<i>Observed frequencies (cm⁻¹)</i>	<i>Assignment</i>
Compound 1	
3450 s	$\nu_s(\text{O}-\text{H})$
3290 w ; 3120 w	$\nu_s(\text{N}-\text{H})$
2970 m ; 2600 w	$\nu_s(\text{C}-\text{H})$
2350 w ; 2000 w	$\nu_s(\text{C}-\text{N})$
1680 sh	$\delta(\text{N}-\text{H}) \& \delta(\text{O}-\text{H})$
1560 s ; 1400 sh	$\nu_{\text{as}}(\text{C}-\text{N})$ and $\nu_{\text{as}}(\text{C}=\text{C})$
1210 s	$\nu_s(\text{C}-\text{N}) \& \nu_s(\text{C}-\text{C})$
995 m	$\delta(\text{C}-\text{C})$
980 w; 820 sh; 725 s ;490 m	$\gamma(\text{C}-\text{C})$, $\gamma(\text{C}-\text{H})$ and $\gamma(\text{C}-\text{N})$
Compound 2	
3006 sh	$\nu_{\text{as}}(\text{CH}_3) \& \nu_{\text{as}}(\text{CH}_2)$
2977 s	$\nu_s(\text{CH}_3)$
2940 sh ; 2758 vw ; 2595 vw	$\nu_s(\text{CH}_2)$
2258 w	$\nu_{\text{as}}(\text{C}-\text{N}) \& \text{CH}_2 \text{ twisting / r(CH}_3)$
1451 s	$\delta_{\text{as}}(\text{CH}_2)$
1393 s ; 1370 sh ; 1269 m	$\delta_s(\text{CH}_3)$
1179 s	r CH ₃ rocking
1114 vw ; 1076 m	$\nu_{\text{as}}(\text{C}-\text{C})$
1025 sh ; 996 sh	$\nu_{\text{as}}(\text{C}-\text{N})$
893 vw	r CH ₂ rocking
782 vs	$\nu_s(\text{C}-\text{N})$
666 vw	$\delta_{\text{as}}(\text{C}-\text{C}-\text{N})$
467 w	$\delta_s(\text{C}-\text{C}-\text{N})$

NB. vs : very strong, s: strong, m: medium, w: weak, vw: very weak and sh: shoulder.

3 References

- 1** M. Ben Nasr, F. Lefebvre and C. Ben Nasr, *Am. J. Anal. Chem.*, 2015, **6**, 446-456
- 2** Y.-L. Hu, J.-H. Lin, S. Han, W.-Q. Chen, L.-L. Yu, D.-D. Zhou, W.-T. Yin, H.-R. Zuo, J.-R. Zhou, L.-M. Yang and C-L. Ni, *Synthetic Metals*, 2012, **162**, 1024-1029
- 3** M. K. Johnson, *John Wiley & Sons, Inc* 215, USA, New York, 2004.
- 4** A. Ouasri, A. Rhandour, M. C. Dhamelincourt, P. Dhamelincourt, A. Mazzah and M. Taibi, *Phase Transitions*, 2003, **76**, 701–709.
- 5** K. Ben Brahim, M. Ben Gzaiel, A. Oueslati and M. Gargouri, *RSC advances* 2018, **8**, 40676-40686.